PHYSICAL REVIEW B **93**, 241114(R) (2016)

Time-resolved photoemission of Sr_2IrO_4

C. Piovera,[1] V. Brouet,[2] E. Papalazarou,[2] M. Caputo,[2] M. Marsi,[2] A. Taleb-Ibrahimi,[3] B. J. Kim,[4] and L. Perfetti[1]

[1]*Laboratoire des Solides Irradiés, Ecole Polytechnique, CNRS, CEA, Université Paris-Saclay, 91128 Palaiseau, France*

[2]*Laboratoire de Physique des Solides, CNRS, Univ. Paris-Sud, Université Paris-Saclay, 91405 Orsay Cedex, France*

[3]*Synchrotron SOLEIL, L'Orme des Merisiers, Saint-Aubin-BP 48, F-91192 Gif sur Yvette, France*

[4]*Max Planck Institute for Solid State Research, Heisenbergstraße 1, D-70569 Stuttgart, Germany*

(Received 16 March 2016; revised manuscript received 29 May 2016; published 23 June 2016)

We investigate the temporal evolution of electronic states in strontium iridate Sr_2IrO_4. The time-resolved photoemission spectra of the intrinsic, electron-doped, and hole-doped samples are monitored in identical experimental conditions. Our data on the intrinsic and electron-doped samples, show that doublon-holon pairs relax near to the chemical potential on a time scale shorter than 70 fs. The subsequent cooling of low-energy excitations takes place in two steps: a rapid dynamics of ≅120 fs is followed by a slower decay of ≅1 ps. The reported time scales endorse the analogies between Sr_2IrO_4 and copper oxides.

DOI: 10.1103/PhysRevB.93.241114

The layered Sr_2IrO_4 is an ideal system to explore electronic correlations, electron-phonon coupling, and antiferromagnetic ordering. Strontium iridate is a quasi-two-dimensional compound with a partially filled $5d$ shell and moderate Coulomb repulsion. In spite of the large extension of $5d$ orbitals, the subtle interplay of spin-orbit interaction, crystal field splitting, and antiferromagnetic interaction leads to an insulating state [1,2]. Due to superexchange interaction, the ground state of Sr_2IrO_4 holds canted antiferromagnetic ordering of the spins on a squared lattice [3]. As in the case of copper oxides [4], the paramagnetic insulator can be viewed as an intermediate Mott-Slater system that is stabilized by short-range correlations of the antiferromagnetic order [5]. The analogy with cuprates can be pushed further [6,7], insofar as doped Sr_2IrO_4 is considered a promising candidate to observe high-temperature superconductivity [8].

It is worth questioning whether iridates and cuprates display the same dynamical behavior upon photoexcitation. In this respect, the insulating copper oxides have already been characterized by exhaustive experiments of transient absorption [9]. Okamoto *et al.* measured at different probing frequencies, thereby disentangling the Drude component from the midgap response. It follows that midgap states arise on a time scale of 40 fs and experience an initial decay within 200 fs. The iridates seem to display a similar response, although the reported experiments have been performed with probing energy exceeding the optical gap value [10,11]. Hsieh *et al.* observed a biexponential kinetic and analyzed the effects of the magnetic transition on the relaxation time [10].

The purpose of this work is to directly follow the relaxation of electronic states in Sr_2IrO_4. We report a time-resolved photoemission experiment of the intrinsic and chemically doped samples. Our data indicate that doublon-holon pairs are highly unstable against the formation of midgap states. The dynamics of such emerging excitations follow a biexponential law that is compatible to the transient absorption reported in La_2CuO_4 [9]. Our results provide further insights on the ultrafast electron relaxation in quasi-two-dimensional Mott insulators with strong antiferromagnetic coupling and reinforce the analogies between iridates and cuprates.

Methods. Samples have been synthesized by a self-flux method [3]. Electron doping is obtained by substituting 3% of the Sr atoms with La, whereas hole doping is done by replacing 15% of Sr atoms with Rh. The crystals have been characterized by x-ray diffraction, resistivity, magnetization measurements, and angle-resolved photoelectron spectroscopy (ARPES). The ARPES measurements have been acquired at the Cassiopée beamline of Synchrotron Soleil. Time-resolved photoemission experiments were performed on the FemtoARPES setup [12], using a Ti:sapphire laser system delivering 35 fs pulses at 1.55 eV (780 nm) with 250 kHz repetition rate. Part of the laser beam is used to generate 6.3 eV photons through cascade frequency mixing in BaB_2O_4 (BBO) crystals. The 1.55 and 6.3 eV beams are employed to photoexcite the sample and induce photoemission, respectively. The energy resolution is ≅60 meV (limited by the energy bandwidth of the UV pulses) and the temporal resolution is ≅60 fs. All the laser photoemission measurements were performed at room temperature and at the base pressure of 7×10^{-11} mbar.

Samples characterization. Figures 1(a) and 1(b) show examples of the resistivity and magnetization measurements in three different samples. The intrinsic Sr_2IrO_4 exhibits an insulating behavior with an activation energy of 30–70 meV. Upon chemical doping, the conductivity drops by two orders of magnitude. The magnetic phase transition is barely visible at electron doping (3% La) and it vanishes at hole doping (15% Rh).

According to the literature, the lower Hubbard band has orbital character $J_{\text{eff}} = 1/2$ and reaches the nearest distance from the chemical potential at the X point of the Brillouin zone [1,13] (we recall that the space group of Sr_2IrO_4 is $I41/acd$). Figure 1(c) shows the energy distribution curves (EDCs) of the X point acquired at the Cassiopée beamline with photon energy of 100 eV, temperature of 50 K, and pressure of 2×10^{-10} mbar. Notice that the Hubbard peak is at ≅ − 0.25 eV in the intrinsic sample and shifts to ≅ − 0.6 eV after La substitution [13]. Upon hole doping (15% Rh), the peak of the $J_{\text{eff}} = 1/2$ band moves at ≅ − 0.1 eV from the chemical potential, giving rise to a small pseudogap instead of a quasiparticle crossing. As explained in our recent ARPES work [13], we can estimate a Mott gap of 0.6–0.7 eV from the difference of the $J_{\text{eff}} = 1/2$ position in hole-doped and electron-doped compounds. This value is consistent with scanning tunneling spectroscopy (STS)

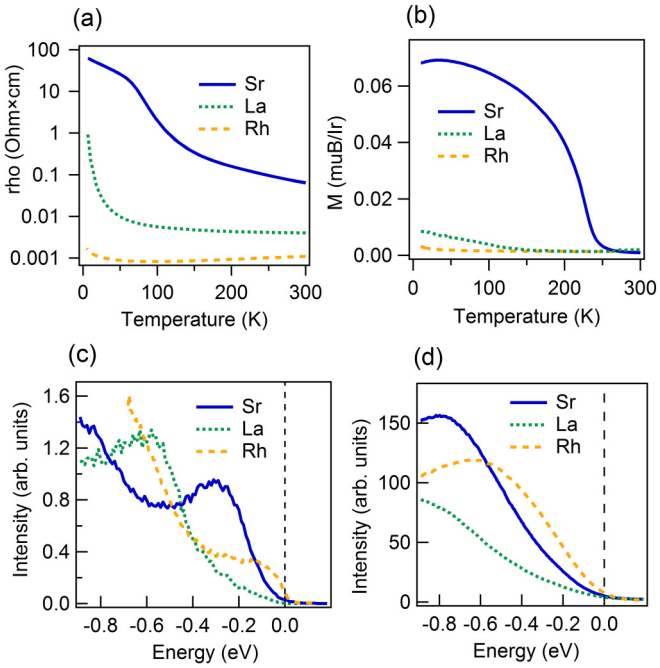

FIG. 1. In-plane resistivity (a) and magnetization curves (b) of intrinsic and doped Sr_2IrO_4. EDCs acquired at the X point of the Brillouin zone with photon energy of 100 eV (c) and acquired at the center of the Brillouin zone with photon energy of 6.3 eV (d). The intrinsic (solid line), electron-doped (dotted line), and hole-doped (dashed line) compounds are marked by the notations Sr, La, and Rh, respectively.

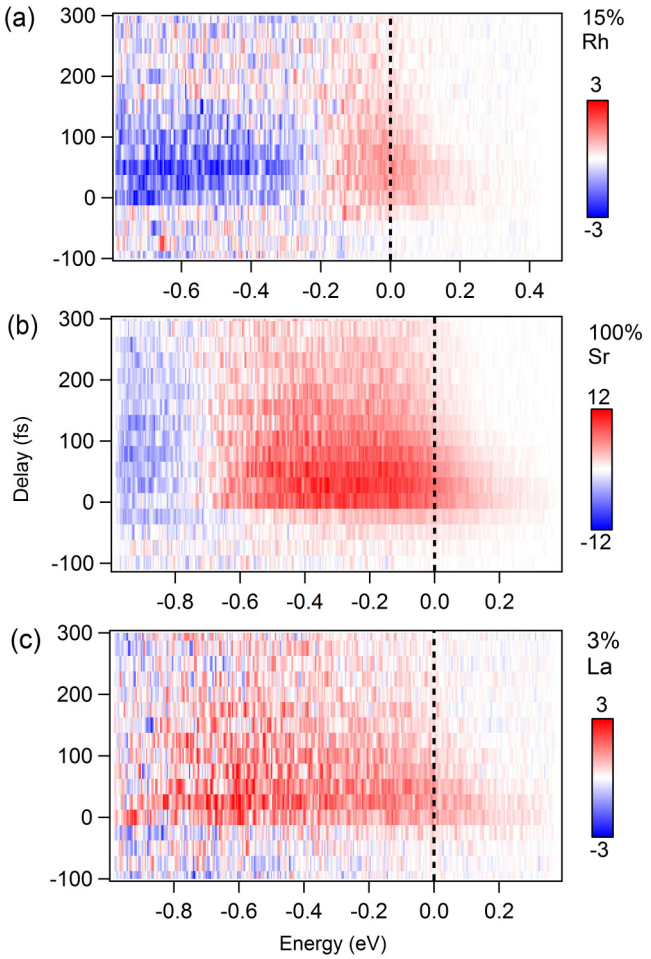

FIG. 2. Map of the pump-on minus pump-off signal acquired with 6.3 eV photons as a function of energy and pump-probe delay. The intensity is normalized with respect to the photon flux and the pump fluence has been set to $\cong 0.7$ mJ/cm^2. Data on Rh-substituted, intrinsic, and La-substituted samples are shown in panels (a), (b), and (c), respectively.

measurements on sample regions with no defects [14,15]. The presence of defects is an unavoidable complexity that has a strong impact on the low-energy physics of iridates [13–16]. STS experiments confirmed that defects induce a local collapse of the Mott gap [14] and established a relation between midgap states and oxygen impurities [15].

Finally, we show in Fig. 1(d) the EDCs acquired with 6.3 eV photon energy at the center of the Brillouin zone and normalized to the photon flux (therefore the relative EDC intensity is not arbitrary). In the intrinsic sample, the direct photoemission from the $J_{\rm eff} = 1/2$ band and the weak umklapp of the $J_{\rm eff} = 3/2$ band should peak at electron energy -1.2 and -0.5 eV, respectively [1,13]. However, the signal in Fig. 1(d) mainly arises from photoelectronic emission assisted by surface roughness and/or from localized states. Accordingly, we verified that EDCs acquired with 6.3 eV photon energy are dispersionless when scanning the emission angle from 0° to 30°. It is reasonable to assume that the EDCs of Fig. 1(d) provide a rough indication of the electron-removal spectral function integrated over the wave-vector index. In agreement with this assumption, we observe a large shift of spectral weight upon electron or hole doping.

Properties of the photoexcited state. Exact diagonalization calculations indicate that the $J_{\rm eff} = 1/2$ electron-hole continuum covers the interval 0.5–1.5 eV [17]. One may expect that upon pumping with 1.55 eV photons, the photoexicted electrons would accumulate in the form of doublon-holon pairs at the bottom of the lower Hubbard band. However, this scenario is in sharp contrast with our experimental results. Figure 2 reports the pump-on minus pump-off EDCs acquired on different samples as a function of delay time. The differential intensity is plotted on a color scale where blue and red stand for photoinduced reduction and increase of photoelectron yield, respectively. Intensity maps of Figs. 2(a), 2(b), and 2(c) have been acquired on Rh-substituted, intrinsic, and La-substituted compounds. We employed a pumping fluence of 0.7 mJ/cm^2, leading to ~ 0.04 excitations per iridium atom. The data indicate that photoexcited electrons do not accumulate in the upper Hubbard band but relax in electronic states near to the chemical potential. This finding is in contrast to recent time-resolved photoemission measurements of the Mott insulator UO_2 [18]. We recall that Sr_2IrO_4 and UO_2 differ in terms of dimensionality, gap size, and impact of the antiferromagnetic correlations. Therefore, two possible scenarios may explain the distinct electron dynamics in these compounds. First, the Sr_2IrO_4 has a Mott gap (0.6 eV) much smaller than that of UO_2 (2.3 eV) [18]. Therefore the rate of multiphonon and multimagnon emission [19,20] could be strong enough to relax electrons across the correlation gap

of Sr_2IrO_4, whereas it may be negligible in UO_2. Second, we know from STS data [14,15] that defects locally disrupt the narrow Mott gap of Sr_2IrO_4. As a consequence, the excited electrons may find viable paths to relax from the upper Hubbard band down to lower lying energies.

We outline in Figs. 2(a)–2(c) that a photoinduced increase of photoemission yield extends well below the chemical potential. A combination of intrinsic and extrinsic effects can explain this finding. On one hand, an intrinsic increase of spectral weight between the lower Hubbard band and the chemical potential is expected because of the partial filling of the Mott gap. This behavior has been observed in $1T$-TaS_2 at comparable excitation densities and should be a general property of Mott insulators with narrow gap [21,22]. On the other hand, an extrinsic and time dependent shift of the EDC can arise from the sudden change of dielectric properties at the surface of the sample. We already observed spectral shift generated by local fields in copper oxides [23], small gap semiconductors [24], and semimetals [25]. As in the case of surface photovoltage, we expect the energy displacement to be more important in the intrinsic compound than in samples with Rh or La substitutions. Future experiments with high harmonic sources [18,26] could access the X point of the Brillouin zone and may shed light on this issue.

Dynamics of the electrons. Figure 3(a) shows pump-on minus pump-off EDCs acquired in the intrinsic sample, at delay time of 25 fs and different pumping fluences. The curves have similar shape and are nearly proportional to the pumping fluence. Therefore, the photoexcited state is still far from the saturation regime of a collapsed Mott insulator [22]. We show in Fig. 3(b) the pump-on minus pump-off EDCs of the intrinsic sample acquired with excitation fluence of 0.7 mJ/cm^2 at different pump-probe delays. Notice that electrons at excitation energy higher than $\cong$0.1 eV follow an exponential distribution $\exp(-\epsilon/kT_e)$ with temperature scale T_e attaining a maximal value of 1900 K. In order to gain further insights on the electronic relaxation, we plot in Fig. 3(c) the temporal evolution of the signal integrated in the energy interval [0.1,0.2] eV. This spectral region is below the upper Hubbard band and above the chemical potential. Therefore the transient signal recorded in [0.1,0.2] eV is an excellent indicator of the energy flow from doublon-holon pairs into lower energy excitations. A fit accounting for the cross-correlation between the pump and probe beam provides the decay time $\tau_1 \cong 70$ fs. This time scale does not change with respect to photoexcitation density and indicates that doublon-holon pairs relax near the chemical potential on a very short time scale. Our results are in line with the sudden decay of the Drude response observed by Okamoto *et al.* in photoexcited cuprates [9].

Next we turn on the temporal evolution of the pump-probe signal in the spectral region where midgap states accumulate. We cannot resolve any finite rise time in the pump-probe signal, indicating that midgap states are formed within less than 60 fs. Figure 3(d) shows the evolution of the photoelectron intensity integrated in the spectral range [−0.1,0] eV. The relaxation of the midgap signal follows a biexponential decay with time constant $\tau_2 \cong 120$ fs and $\tau_3 \cong 1$ ps. As shown in Fig. 3(e), the presence of the two time scales is clearly resolved by plotting the decay curve on a logarithmic scale. Similar dynamics

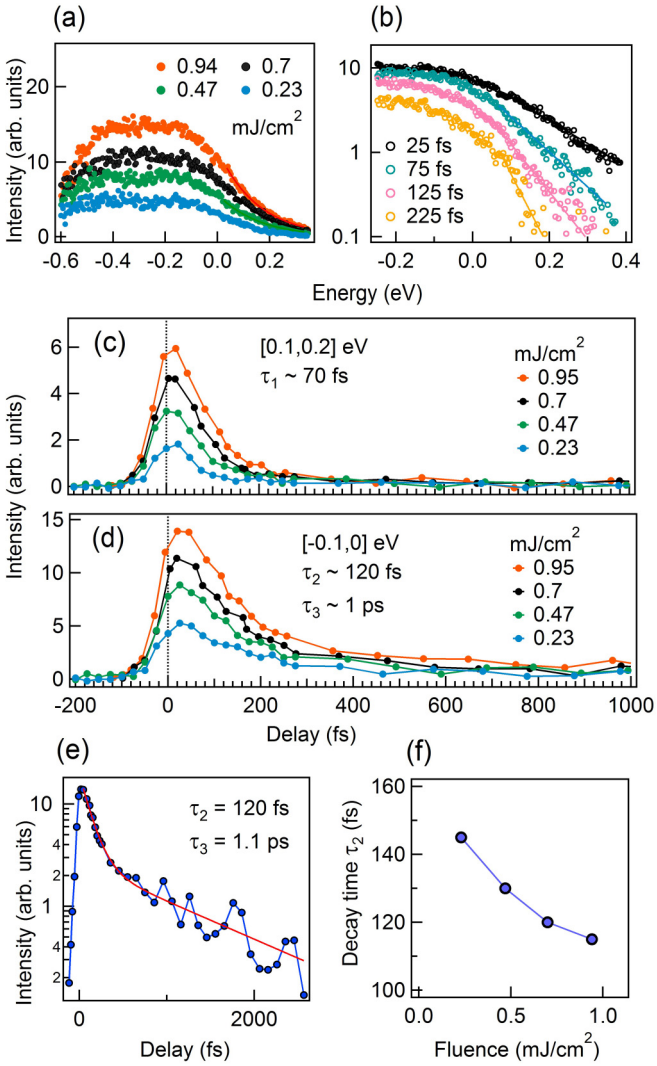

FIG. 3. All data of this figure refer to the intrinsic sample. (a) Energy distribution of the pump-on minus pump-off signal acquired at delay time of 25 fs at different pumping fluence. (b) Energy distribution of the pump-on minus pump-off signal acquired with 0.7 mJ/cm^2 at different pump-probe delays. The solid lines stand for the exponential fit of the spectral tail at energy $\geqslant$0.1 eV. Evolution of the signal integrated in the energy interval [0.1,0.2] eV [panel (c)] and [−0.1,0] [panel (d)] as a function of delay time and for different fluences. (e) Logarithmic plot of the [−0.1,0] eV signal for pump fluence of 0.7 mJ/cm^2. (f) Dependence of the decay time τ_2 on the pump fluence.

have been also reported in experiments of transient reflectivity at 1.5 eV [10]. Most importantly, we outline here the clear analogy between iridates and cuprates. According to Okamoto *et al.*, the midgap states of photoexcited La_2CuO_4 display an initial relaxation taking place within 200 fs [9]. Such fast recovery of the charge gap is typical of quasi-two-dimensional Mott insulators with strong antiferromagnetic correlations, whereas this does not take place in correlated insulators where the partial gap filling comes along with large structural distortions [27,28].

As in the case of cuprates [9,23,29], we ascribe the τ_2 decay to the energy dissipation via emission of optical phonons or

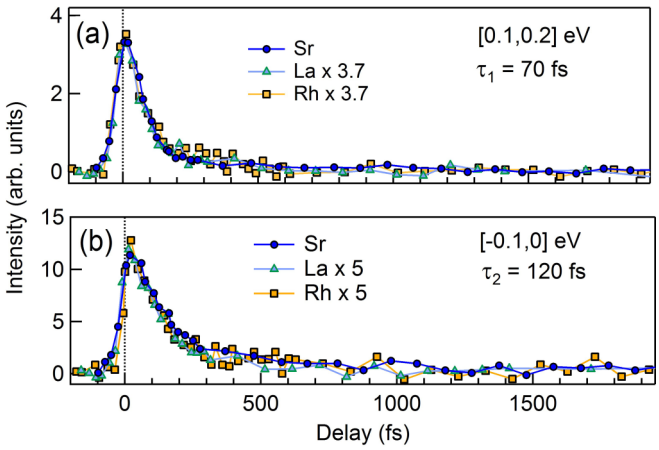

FIG. 4. Evolution of the pump-probe signal integrated in the energy interval [0.1,0.2] eV [panel (a)] and [−0.1,0] [panel (b)]. The circles, triangles, and squares stand for the intrinsic, La-substituted, and Rh-substituted samples.

localized vibrations. The slower dynamics τ_3 is instead due to lattice anharmonicity and acoustic phonon emission. Within our experimental accuracy we could not observe any fluence dependence in the slow time scale τ_3. Conversely, Fig. 3(f) shows a weak increase of τ_2 by lowering the photoexcitation density. Lastly, Fig. 4 compares the dynamics of the signal acquired on the intrinsic, Rh-substituted, and La-substituted samples. Strikingly, we observe an identical temporal behavior in the three different samples. Independently of the doping, the excited electrons integrated in the interval [0.1,0.2] eV decay with time constant $\tau_1 = 70$ fs. Instead, the midgap states in the energy window [−0.1,0] eV follow a biexponential decay with time constants $\tau_2 = 120$ fs and $\tau_3 = 1.1$ ps.

In conclusion, time-resolved photoemission measurements of Sr_2IrO_4 reveal the electron dynamics upon photoexcitation above the band gap. The photoexcited holon-doublon pairs decay into midgap states on an ultrafast time scale. Presumably, this behavior arises from the emission of collective excitations and defect mediated decay. We report identical dynamics in the intrinsic and doped compounds, suggesting that metallicity and screening do not influence the relaxation of the photoexcited electrons. Our time-resolved photoemission data of iridates are in good agreement with optical experiments on copper oxides, providing compelling evidence of common dynamics in these intermediate Mott-Slater insulators.

Acknowledgments. We acknowledge S. Biermann, M. Ferrero, and M. Eckstein for enlightening discussions on the physics of Mott insulators and iridates. This work is supported by Investissements d'Avenir LabEx PALM (Grant No. ANR-10-LABX-0039PALM), by the EU/FP7 under the contract Go Fast (Grant No. 280555), and by the Région Ile-de France through the program DIM OxyMORE.

[1] B. J. Kim, Hosub Jin, S. J. Moon, J.-Y. Kim, B.-G. Park, C. S. Leem, Jaejun Yu, T. W. Noh, C. Kim, S.-J. Oh, J.-H. Park, V. Durairaj, G. Cao, and E. Rotenberg, Phys. Rev. Lett. **101**, 076402 (2008).

[2] C. Martins, M. Aichhorn, L. Vaugier, and S. Biermann, Phys. Rev. Lett. **107**, 266404 (2011).

[3] B. J. Kim, H. Ohsumi, T. Komesu, S. Sakai, T. Morita, H. Takagi, and T. Arima, Science **323**, 1329 (2009).

[4] A. Comanac, L. de Medici, M. Capone, and A. J. Millis, Nat. Phys. **4**, 287 (2008).

[5] H. Watanabe, T. Shirakawa, and S. Yunoki, Phys. Rev B **89**, 165115 (2014).

[6] Y. K. Kim, O. Krupin, J. D. Denlinger, A. Bostwick, E. Rotenberg, Q. Zhao, J. F. Mitchell, J. W. Allen, and B. J. Kim, Science **345**, 187 (2014).

[7] A. de la Torre, S. McKeown Walker, F. Y. Bruno, S. Riccó, Z. Wang, I. Gutierrez Lezama, G. Scheerer, G. Giriat, D. Jaccard, C. Berthod, T. K. Kim, M. Hoesch, E. C. Hunter, R. S. Perry, A. Tamai, and F. Baumberger, Phys. Rev. Lett. **115**, 176402 (2015).

[8] Y. K. Kim, N. H. Sung, J. D. Denlinger, and B. J. Kim, Nat. Phys. **12**, 37 (2016).

[9] H. Okamoto, T. Miyagoe, K. Kobayashi, H. Uemura, H. Nishioka, H. Matsuzaki, A. Sawa, and Y. Tokura, Phys. Rev. B **83**, 125102 (2011).

[10] D. Hsieh, F. Mahmood, D. H. Torchinsky, G. Cao, and N. Gedik, Phys. Rev. B **86**, 035128 (2012).

[11] Z. Alpichshev, F. Mahmood, G. Cao, and N. Gedik, Phys. Rev. Lett. **114**, 017203 (2015).

[12] J. Faure, J. Mauchain, E. Papalazarou, W. Yan, J. Pinon, M. Marsi, and L. Perfetti, Rev. Sci. Instrum. **83**, 043109 (2012).

[13] V. Brouet, J. Mansart, L. Perfetti, C. Piovera, I. Vobornik, P. Le Fèvre, F. Bertran, S. C. Riggs, M. C. Shapiro, P. Giraldo-Gallo, and I. R. Fisher, Phys. Rev. B **92**, 081117(R) (2015).

[14] Y. Okada, D. Walkup, H. Lin, C. Dhital, T.-R. Chang, S. Khadka, W. Zhou, H.-T. Jeng, M. Paranjape, A. Bansil, Z. Wang, S. D. Wilson, and V. Madhavan, Nat. Mater. **12**, 707 (2013).

[15] J. Dai, E. Calleja, G. Cao, and K. McElroy, Phys. Rev. B **90**, 041102 (2014).

[16] A. Glamazda, W.-J. Lee, K.-Y. Choi, P. Lemmens, H. Y. Choi, N. Lee, and Y. J. Choi, Phys. Rev. B **89**, 104406 (2014).

[17] B. H. Kim, G. Khaliullin, and B. I. Min, Phys. Rev. Lett. **109**, 167205 (2012).

[18] S. M. Gilbertson, T. Durakiewicz, G. L. Dakovski, Y. Li, J.-X. Zhu, S. D. Conradson, S. A. Trugman, and G. Rodriguez, Phys. Rev. Lett. **112**, 087402 (2014).

[19] Z. Lenarcic and P. Prelovsek, Phys. Rev. B **90**, 235136 (2014).

[20] Z. Lenarcic, M. Eckstein, and P. Prelovsek, Phys. Rev. B **92**, 201104(R) (2015).

[21] L. Perfetti, P. A. Loukakos, M. Lisowski, U. Bovensiepen, H. Berger, S. Biermann, P. S. Cornaglia, A. Georges, and M. Wolf, Phys. Rev. Lett. **97**, 067402 (2006).

[22] L. Perfetti, P. A. Loukakos, M. Lisowski, U. Bovensiepen, H. Berger, S. Biermann, A. Georges, and M. Wolf, New J. Phys. **10**, 053019 (2008).

[23] C. Piovera, Z. Zhang, M. d'Astuto, A. Taleb-Ibrahimi, E. Papalazarou, M. Marsi, Z. Z. Li, H. Raffy, and L. Perfetti, Phys. Rev. B **91**, 224509 (2015).

[24] J. Mauchain, Y. Ohtsubo, M. Hajlaoui, E. Papalazarou, M. Marsi, A. Taleb-Ibrahimi, J. Faure, K. A. Kokh, O. E. Tereshchenko, S. V. Eremeev, E. V. Chulkov, and L. Perfetti, Phys. Rev. Lett. **111**, 126603 (2013).

[25] E. Papalazarou, J. Faure, J. Mauchain, M. Marsi, A. Taleb-Ibrahimi, I. Reshetnyak, A. van Roekeghem, I. Timrov, N. Vast, B. Arnaud, and L. Perfetti, Phys. Rev. Lett. **108**, 256808 (2012).

[26] S. Hellmann, T. Rohwer, M. Kalläne, K. Hanff, C. Sohrt, A. Stange, A. Carr, M. M. Murnane, H. C. Kapteyn, L. Kipp, M. Bauer, and K. Rossnagel, Nat. Commun. **3**, 1069 (2012).

[27] V. Brouet, J. Mauchain, E. Papalazarou, J. Faure, M. Marsi, P. H. Lin, A. Taleb-Ibrahimi, P. Le Fèvre, F. Bertran, L. Cario, E. Janod, B. Corraze, V. T. Phuoc, and L. Perfetti, Phys. Rev. B **87**, 041106(R) (2013).

[28] R. Yoshida, T. Yamamoto, Y. Ishida, H. Nagao, T. Otsuka, K. Saeki, Y. Muraoka, R. Eguchi, K. Ishizaka, T. Kiss, S. Watanabe, T. Kanai, J. Itatani, and S. Shin, Phys. Rev. B **89**, 205114 (2014).

[29] L. Perfetti, P. A. Loukakos, M. Lisowski, U. Bovensiepen, H. Eisaki, and M. Wolf, Phys. Rev. Lett. **99**, 197001 (2007).